Possible charge inhomogeneities in the CuO_2 planes of $YBa_2Cu_3O_{6+x}$ ($x=0.25,0.45,0.65,0.94$) from pulsed neutron diffraction

M. Gutmann and S. J. L. Billinge
Department of Physics and Astronomy and Center for Fundamental Materials Research, Michigan State University, East Lansing, Michigan 48824-1116

E. L. Brosha and G. H. Kwei
Los Alamos National Laboratory, Los Alamos, New Mexico 87545

(Received 25 August 1999)

The atomic pair distribution functions (PDFs) of four powder samples of $YBa_2Cu_3O_{6+x}$ ($x=0.25,\ 0.45,\ 0.65,\ 0.94$) at 15 K have been measured by means of pulsed neutron diffraction. The PDF is modeled using a full-profile fitting approach to yield structural parameters. In contrast to earlier x-ray absorption fine structure work we find no evidence of a split apical oxygen site. However, a slightly improved fit over the average crystallographic model results when the planar Cu(2) site is split along the *c* direction. This is interpreted in terms of charge inhomogeneities in the CuO_2 planes.

I. INTRODUCTION

The observation of charge stripes[1] in $La_{2-x-y}Nd_ySr_xCuO_4$ raises the interesting possibility that inhomogeneous charge distributions in general, and stripes in particular, are a generic phenomenon of high-temperature superconductors. Charge stripes give rise to local structural distortions which can be evident using local structural probes. For example, both atomic pair distribution function (PDF) analysis on neutron powder diffraction data[2,3] and extended x-ray absorption fine structure[4] (XAFS) indicate that in the $La_{2-x}Sr_xCuO_4$ system local structural distortions exist which are consistent with such charge inhomogeneities. It is clearly important to establish their presence more widely in the high-temperature superconductors.

A long-standing controversy exists between the diffraction and XAFS communities concerning the existence of a double-well potential for the apical, O(4), ion in $YBa_2Cu_3O_{6+x}$ (123). This was first reported from XAFS data[5,6] as a double well with the minima of the wells separated along the *c* direction by 0.13 Å. It was also reported that the well structure becomes modified close to T_c.[5–7] The controversy arose because this result seemed to contradict single-crystal[8,9] and powder diffraction[10–13] data which gave no evidence of enlarged thermal factors for O(4) along the *c* direction as would be expected if such a double well existed. In addition, the XAFS result[14] predicts an anomalously short Cu(1)-O(4) bond [Cu(1) is the chain copper] which seems to be questionable on chemical grounds. Nonetheless, subsequent XAFS studies have consistently reproduced the main result: that the Cu(1)-O(4) and Cu(2)-O(4) pair distributions from the data are best modeled as each having two equally populated components separated by ~ 0.1 Å.[15–17] There appears to be no correlation between superconducting properties and the observation of the split position.[15–17] Also, the split Cu-O(4) correlations are not present in all samples.[15,16] The importance of this structural feature to the superconductivity is clearly doubtful; however, a solution to this controversy may elucidate important information about the properties of these materials, especially in light of the significant evidence that lattice effects are important in the superconductors.[14,18]

We have taken a different approach to study this problem. We have made an atomic pair distribution function analysis of neutron powder diffraction data. The PDF technique is a diffraction technique which, nonetheless, reveals local atomic structure directly.[19] In this sense it bridges the diffraction and local structure domains. We would expect the PDF to reflect the atomic pair distributions observed with XAFS whereas a conventional Rietveld analysis of the same data set should recover the crystallographic result.

In the PDF technique the total scattering data are measured including both Bragg and diffuse scattering. These data are Fourier transformed into real space, yielding the PDF directly. There are two main advantages of this approach over XAFS. First, the data reduction to obtain the PDF is straightforward and deductive and results in a virtually undistorted, high-resolution, PDF. This can also be recovered from XAFS data, but only by careful fitting procedures.[16,20] Second, the PDF is obtained over a wide range of atomic separation, *r*. This allows data modeling to be carried out over an extended range of the PDF which puts more constraints on possible data interpretations and makes structural solutions more (though not completely) unique. The disadvantage with respect to XAFS of the present study is that the total PDF is measured rather than a chemical specific PDF which has fewer atom pairs contributing to the observed PDF. Also, most XAFS studies relating to this question were made on oriented samples with a polarized beam which further reduces the number of correlations in the resulting PDF.[5–7,15–17] While this kind of analysis is, in principle, possible using diffraction[19] it has not been done.

We have measured PDFs from four samples of $YBa_2Cu_3O_{6+x}$ with $x=0.25,\ 0.45,\ 0.65,\ 0.94$ at 15 K. These were analyzed using PDFFIT,[21] a full-profile fitting program analogous to Rietveld refinement but which fits the PDF and therefore yields local structural information.[22] The resulting

 ©2000 The American Physical Society

structural parameters are in good agreement with the average crystal structure; in particular we refine a thermal factor on the O(4) site which is not unphysically large. We have attempted to refine split positions on O(4) without success. However, we do refine a split position along c on the in-plane copper site which results in a small improvement in agreement. We interpret this observation in terms of an inhomogeneous charge distribution in the CuO_2 plane consistent with the presence of localized charges, for example, as would be expected in the presence of charge stripes.

II. EXPERIMENT

The $YBa_2Cu_3O_{6+x}$ samples were prepared using standard solid-state reaction methods. Stochiometric quantities of CuO, $BaCO_3$, and Y_2O_3 were ground in an Al_2O_3 mortar and pestle under acetone until well mixed. The sample was air dried, and the powder contents were loaded into a 3/4-in-diameter steel die and uniaxially pressed at 1000 lb. The pellet sample was removed and placed into an alumina boat. The sample was placed into a preheated (800 °C) tube furnace under 1 atm of flowing oxygen. The furnace tube was sealed and the furnace temperature was immediately raised to 960 °C. The sample was fired for 72 h and quenched. After cooling to room temperature, the sample was removed, ground under acetone, and repressed. This firing cycle was repeated until the powder x-ray diffraction (XRD) traces showed no evidence of the presence of second phases. The typical reaction time was on the order of 1 week. Fully oxidized YBCO ($x=0.94$) was prepared by heating a portion of the YBCO sample to 450 °C in 1 atm PO_2. The sample was cooled to room temperature at a rate of 2 °C/min and at 1 atm PO_2.

The oxygen nonstoichiometric YBCO samples were prepared using data from Kishio *et al.*[23] Portions of the first YBCO sample were divided and placed into separate alumina boats. The annealing temperature and PO_2 were determined from Kishio *et al.* as set by the desired oxygen content for each sample. An Ametek oxygen analyzer was used to set the oxygen content of the annealing gas mixture as determined from the furnace exhaust while the furnace was at room temperature. The oxygen concentration was maintained by diluting a 20% O_2/Ar balance gas mixture with Ar. Each sample was annealed at the selected temperature until the oxygen content of the exhaust gas returned the concentration that was intially set by the mixing manifold. Typically, upon heating, the samples would lose oxygen and this would cause a spike in the measured oxygen concentration. After equilibration, the boat was quenched to room temperature under the controlled PO_2 atmosphere with the aid of a Pt wire that passed through a septum cap to the furnace tube exterior. Thus the atmosphere inside the furnace was maintained during the entire anneal and subsequent quench to room temperature.

The oxygen stoichiometry of each sample was determined by reduction of the sample in 6% H_2/Ar forming gas. The thermogravimetric analysis (TGA) scans were made at 5 °C/min to a maximum temperature of 1100 °C. The gas flow rate was 80 ml/min. A high-resolution Siemens D5000 powder x-ray diffractometer using Cu $K\alpha$ radiation and an incident beam monochrometer were used for XRD. A Perkin/Elmer TGA 7 was used for thermogravimetry.

Neutron powder diffraction data were collected on the High Intensity Powder Diffractometer (HIPD) at the Manuel Lujan Neutron Scattering Center (MLNSC) at Los Alamos National Laboratory for the $x=0.65$ and 0.94 samples and on the Glass, Liquids and Amorphous diffractometer (GLAD) at the Intense Pulsed Neutron Source (IPNS) at Argonne National Laboratory for the $x=0.25$ and 0.45 samples. The samples of about 10 g were sealed in a cylindrical vanadium tube with helium exchange gas. Data were collected at various temperatures between 15 K and room temperature in a closed-cycle helium refrigerator. Additional data sets were collected to account for the scattering from the sample environment and the empty can. A vanadium rod was measured to account for the flux distribution at the sample position. The data are corrected for detector deadtime and efficiency, background, absorption, multiple scattering, and inelasticity effects and normalized with respect to the incident flux and the total sample scattering cross section to yield the total scattering structure function $S(Q)$. This quantity is Fourier transformed according to

$$G(r)=\frac{2}{\pi}\int_0^\infty Q[S(Q)-1]\sin(Qr)dQ. \tag{1}$$

Data collection and analysis procedures have been described elsewhere.[24] Random errors in the data from statistical counting fluctuations are estimated by propagating the errors from the raw data using standard error propagation.[27] The error propagation process has been described in detail elsewhere.[25,26] The reduced structure factor $F(Q)=Q[S(Q)-1]$ from a typical data set is shown in Fig. 1(a). The resulting PDF is shown in Fig. 1(b).

The PDF is a real-space representation of the local structure in the form of pair distances. Modeling of PDF was carried out using the PDFFIT program[21] to perform a least-squares full-profile fit. The structural inputs for the program are atomic positions, occupancies, and anisotropic thermal factors directly analogous to Rietveld refinements, allowing direct comparison of data analyzed in real and reciprocal space. Estimated standard deviations on the refined values are obtained from the variance-covariance matrix in the usual way.[27] Again, we stress that the PDF is being fit and the local structure is obtained from the PDF refinement. This is because the PDF is obtained from both Bragg and diffuse scattering whereas the Rietveld fits include only Bragg scattering. We have also carried out Rietveld refinement of our data in reciprocal space using the program GSAS.[28] and these are compared with the PDF fits. Local distortions away from the average structure are incorporated into the PDF modeling by reducing the symmetry or increasing the size of the unit cell used in the model.

III. RESULTS

A. Comparison with the crystallographic structure

We would like to know if refinements of the PDF reproduce the average crystallographic structure. We compare our refinements with the results of the single-crystal x-ray diffraction study of Schweiss *et al.*[9] The results are shown in Table I. The data are from the the $x=0.94$ sample taken at 90

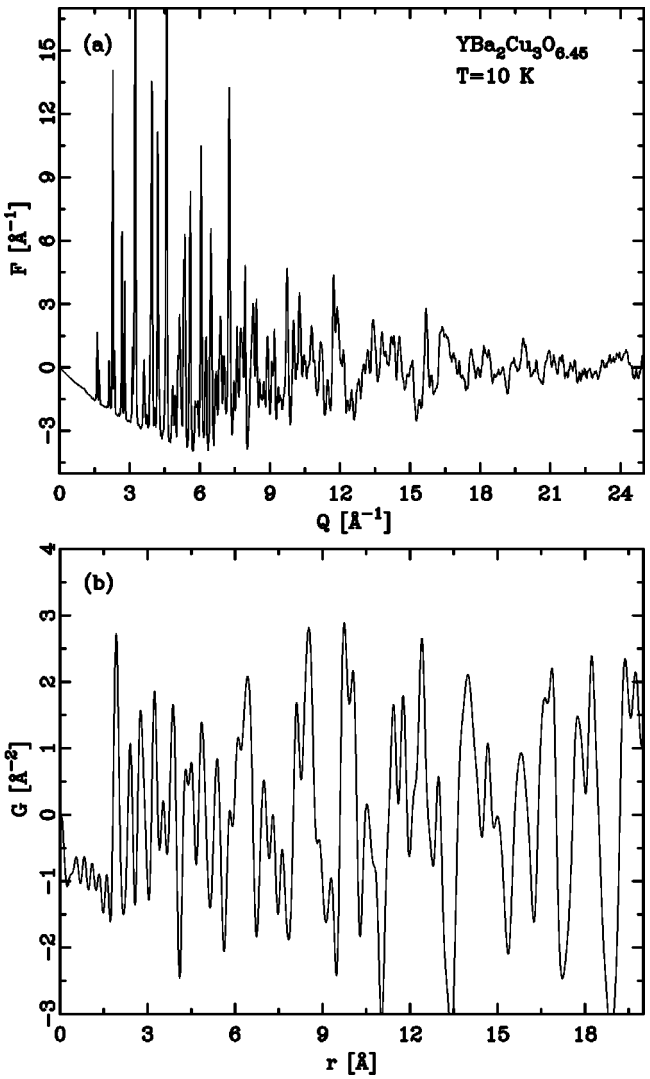

FIG. 1. (a) Reduced structure factor $F(Q)=Q[S(Q)-1]$ for $YBa_2Cu_3O_{6.45}$ measured at 15 K. (b) Reduced radial distribution function, $G(r)$, from the data shown in (a).

K and the constraints on the atomic positional and anisotropic thermal factors were made to mirror those of the single-crystal study. We took two separate data sets at 90 K on cooling and warming. The results from each data set reproduce very well, so only the cooling cycle data-set refinements are reproduced in the table. The agreement with the single-crystal study is clearly very good.

We have also compared our PDF fits with Rietveld refinements of our own data using the GSAS Rietveld package.[28] Again, the agreement is good although the Rietveld refinement produced some unphysical thermal factors. In the case of the PDF fits the data are used over a wider range of Q than the Rietveld fits: $Q_{max}=25$ Å^{-1} for the PDFs and $Q_{max}=15.7$ Å^{-1} ($d=0.4$ Å) for the Rietveld refinements. The qualitative results of the average structure are reproduced in the local structure; for example, U_{33} on the apical oxygen site is small [0.0046(2) (Ref. 30)] in both the Rietveld and PDFFIT refinements. The good agreement between the PDF and crystallographic fits suggests that the difference between the XAFS and crystallographic results cannot be explained simply due to the different length scale of the two measurements.

TABLE I. Comparison between the structural parameters of $YBa_2Cu_3O_{6+x}$ at 90 K obtained from PDF refinements and single-crystal data (Ref. 9). The PDF refinement was carried out over the range $1.5<r<15.27$ Å. The thermal parameters are in units of Å^2. The numbers in parantheses represent one standard deviation on the last digit. The space group used was *Pmmm* with Y on (0.5,0.5,0.5), Ba on (0.5,0.5,z), Cu(1) on (0,0,0), Cu(2) on (0,0,z), O(1) on (0, 0.5, 0), O(2) on (0.5, 0, z), O(3) on (0,0.5,z), and O(4) on (0,0,z).

Parameter	PDF fits	Single crystal Ref. 9
a[Å]	3.8269(6)	3.8202
b[Å]	3.8960(5)	3.8858
c[Å]	11.696(2)	11.696
Y $U_{11}=U_{22}$	0.0028(1)	0.0032(4)
U_{33}	0.0040(2)	0.0016(5)
Ba $U_{11}=U_{22}$	0.0018(1)	0.0046(4)
U_{33}	0.0047(2)	0.0024(5)
z	0.1840(2)	0.18367(12)
Cu(1) $U_{11}=U_{22}$	0.0038(2)	0.0037(5)
U_{33}	0.0025(2)	0.0015(5)
Cu(2) $U_{11}=U_{22}$	0.0020(1)	0.0020(3)
U_{33}	0.0045(2)	0.0029(4)
z	0.3548(2)	0.35466(7)
O(1) U_{11}	0.0136(7)	0.0116(15)
U_{22}	0.0051(4)	0.0055(14)
U_{33}	0.0070(5)	0.0047(11)
Occupation	0.94	0.977(13)
O(2) U_{11}	0.0036(2)	0.0037(4) [a]
U_{22}	0.0048(2)	0.0046(4) [a]
U_{33}	0.0052(2)	0.0045(3)
z	0.3780(3)	0.37818(7)
O(3) U_{11}	0.0048(2)	0.0046(4) [a]
U_{22}	0.0036(2)	0.0037(4) [a]
U_{33}	0.0052(2)	0.0045(4)
z	0.3782(3)	0.37818(7)
O(4) $U_{11}=U_{22}$	0.0043(2)	0.0070(4)
U_{33}	0.0041(2)	0.0041(5)
z	0.1599(2)	0.15918(10)

[a]We have adopted the naming scheme given in Ref. 29 with O(2) at $(\frac{1}{2},0,z)$, O(3) at $(0,\frac{1}{2},z)$. We have converted the atomic positions from Ref. 9 to be consistent with this.

B. Comparison with the XAFS results

In Fig. 2(a) we compare two PDF models which simulate the crystallographic and XAFS models. The PDF calculated using the average crystal structure is shown as a solid line. The dashed line shows the PDF calculated when the O(4) site is split by 0.13 Å along c and each site is occupied 50% as suggested by the XAFS results. All other parameters in the models were kept the same. The difference is shown below. The presence of such a split position clearly has a small but significant effect on the PDF throughout the r range. The magnitude of the signal expected from a split O(4) site is small in the total PDF; however, by fitting over a range of r it should be possible to establish the existence of such a split from the PDF if it exists.

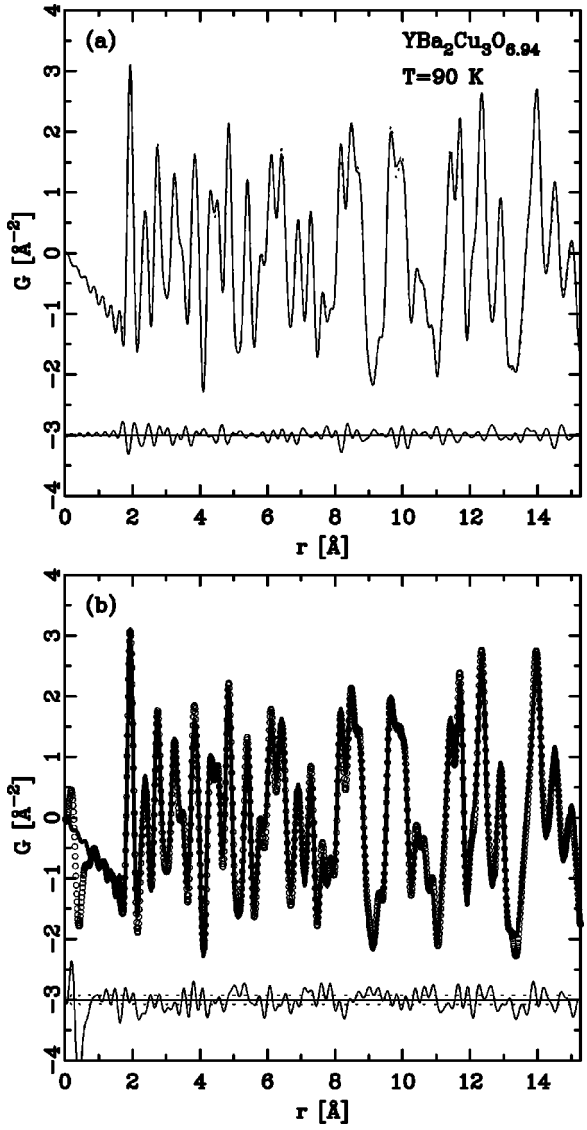

FIG. 2. (a) PDF calculated using the average crystal structure model (solid line) and the XAFS model of Ref. 6 (dashed line). (b) Open symbols: $YBa_2Cu_3O_{6.94}$ 90 K data. Solid line: fit to the data using the average crystal structure model constrained in the same way as the Rietveld refinements. Differences are plotted below.

In Fig. 2(b) we show the data from $x=0.94$, $T=90$ K, as symbols with the PDF from the converged crystallographic model plotted as a solid line. This is the same as the solid line in Fig. 2(a). The difference curve is shown below. If the split site exists in the data but not in the model, which is constrained to have the crystallographic symmetry with no split site, we would expect the two difference curves to be similar. The difference curves appear uncorrelated suggesting qualitatively that the split O(4) site is not present in the data.

C. Search for anharmonic atomic sites

Using PDFFIT we searched for possible split positions in the structure. First, motivated by the XAFS model, we tried refining a split position for the O(4) ion along the *c* direction. Refinements were carried out over the range $1 \leqslant r \leqslant 15$ Å and $1 \leqslant r \leqslant 5$ Å to check the response of the intermediate- and short-range structure. An initial split of 0.1 Å was given to the model, and Δ, the magnitude of the split, was allowed to vary. The occupancy of each split site was set initially to 0.5 but allowed to vary with the constraint that $n_A + n_B = 1.0$ where n_A and n_B are the occupancies of the *A* and *B* sites respectively (see Fig. 3 for details). In both cases Δ refined to a negligible value, again questioning the existence of such a split site.

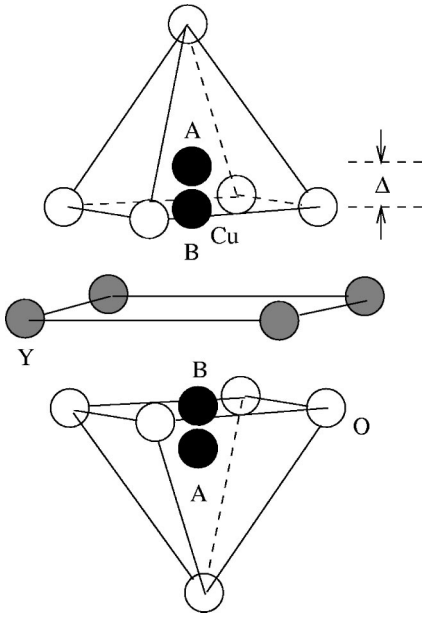

FIG. 3. Illustration of the split Cu(2) site. Two adjacent CuO_5 pyramids are shown. The label for the A site is the same as used in Table III. The size of the split is amplified for clarity.

Based on the crystallographic results we notice that the chain oxygen, O(1), has a large thermal factor along the *a* direction perpendicular to the chain. Also Cu(1), the chain copper, has a relatively large thermal factor perpendicular to the chain. Also, interestingly, the in-plane copper, Cu(2), has a similarly large thermal factor along *c*. We searched for evidence of split atomic sites on each of these atoms in the directions indicated, taking a similar approach to that used for the O(4). Interestingly, the only case where a split site refined to a finite value giving a lower residual was in the case of Cu(2) split along *c*. The results are summarized in Tables II and III. The geometry of the split Cu(2) *c* sites are shown in Fig. 3. The two distinct copper sites are labeled A and B corresponding to sites which are displaced respectively towards and away from the apical oxygen.

For fits over the range to 15.27 Å, refinements to all the data sets were stable and convergent for the split position on Cu(2) along *c* [which was not the case for a split on O(4), for example]; however, the split sometimes refined to a negligibly small value and the improvement in fit is always small and barely significant. The results are much more robust when the fit is confined to the range $1.5 < r < 5.2$. In this case significant improvements in agreement factor are produced when splits in the range $x = 0.10(5) - 0.28(8)$ Å are refined. Refined values from the GLAD data and the HIPD data are self-consistent but there is not quantitative agreement between the results from these two instruments. The GLAD data refine a significantly larger split. This is consistent with the observation in Table II that GLAD thermal factors are

TABLE II. Structural data of $YBa_2Cu_3O_{6+x}$ from the PDF refinements using the average crystallographic structure ($Pmmm$). All data were collected at 15 K. See Table I for atomic positions.

	$x=0.25$	$x=0.45$	$x=0.65$	$x=0.94$
Instrument	GLAD	GLAD	HIPD	HIPD
a	3.8711(3)	3.8556(7)	3.8364(5)	3.8256(7)
b	3.8711(3)	3.8884(7)	3.8965(4)	3.8944(6)
c	11.807(2)	11.749(2)	11.724(1)	11.693(2)
Cu(1) U_{11}	0.0052(2)	0.0053(3)	0.0028(2)	0.0033(2)
U_{22}	0.0052(2)	0.0060(3)	0.0045(3)	0.0012(2)
U_{33}	0.0012(2)	0.0038(2)	0.0025(2)	0.0011(2)
Cu(2) U_{11}	0.0037(1)	0.0025(2)	0.0015(1)	0.0015(1)
U_{22}	0.0037(1)	0.0049(2)	0.0028(1)	0.0021(1)
U_{33}	0.0063(2)	0.0059(2)	0.0039(1)	0.0032(2)
z	0.3594(2)	0.3581(2)	0.3562(2)	0.3564(2)
O(1) U_{11}	0.042(8)	0.030(2)	0.021(1)	0.0092(7)
U_{22}	0.008(3)	−0.0004(6)	0.0027(4)	0.0056(4)
U_{33}	0.018(5)	0.0116(2)	0.0012(2)	0.0062(5)
Occupation	0.25	0.45	0.65	0.94
O(2) U_{11}	0.0050(2)	0.0052(2)	0.0035(1)	0.0023(1)
U_{22}	0.0050(2)	0.0049(2)	0.0046(1)	0.0039(1)
U_{33}	0.0074(2)	0.0064(2)	0.0050(1)	0.0063(2)
z	0.3780(2)	0.3784(3)	0.3791(3)	0.3785(3)
O(3) U_{11}	0.0050(2)	0.0049(2)	0.0046(1)	0.0039(1)
U_{22}	0.0050(2)	0.0052(2)	0.0035(1)	0.0023(1)
U_{33}	0.0074(2)	0.0064(2)	0.0050(1)	0.0063(2)
z(O(3))	0.3780(2)	0.3776(3)	0.3777(3)	0.3781(3)
O(4) U_{11}	0.0073(2)	0.0067(3)	0.0033(3)	0.0020(2)
U_{22}	0.0073(2)	0.0079(3)	0.0081(3)	0.0042(3)
U_{33}	0.0088(3)	0.0073(3)	0.0041(2)	0.0055(2)
z	0.1538(2)	0.1554(2)	0.1580(2)	0.1601(2)
R_w	13.7	13.9	10.9	17.3

consistently larger than those refined from HIPD data. The origin of this is that the GLAD data have a lower real-space resolution. We correct in the modeling for the experimental resolution coming from the finite Q_{max} of the measurement; however, there is an additional loss in real-space resolution which comes from a Q-dependent asymmetric line broadening from time-of-flight spectrometers[31] which is significant in the GLAD data and is not, at present, corrected in the modeling. Thus, we expect the GLAD data to overestimate the split. The most likely value of the split is between 0.1 and 0.2 Å. The observation of disorder on the Cu(2) site but not the apical oxygen site is consistent with another recent differential PDF study on optimally doped $YBa_2Cu_3O_{6+x}$.[32]

TABLE III. Results of the PDF refinement including a split Cu(2) site for various oxygen concentrations x. The PDF refinements were carried out over the ranges $1.5<r<5.2$ Å and $1.5<r<15.27$ Å. Δ is the magnitude of the Cu(2) split along z, n_A is the occupancy of the A site in the split site model (see Fig. 3 for details), and R_{ws} and R_{wu} are the weighted profile residuals for the converged fits, respectively, with and without the Cu split position. The numbers in parantheses represent one standard deviation on the last digit.

	$1.5<r<5.2$ Å				$1.5<r<15.27$ Å			
x	Δ(Å)	n_A	R_{ws}	R_{wu}	Δ(Å)	n_A	R_{ws}	R_{wu}
0.25	0.28(8)	0.14(4)	13.9	15.7	0.01(2)	0.50(3)	13.3	13.7
0.45	0.20(6)	0.25(5)	15.4	16.9	0.17(6)	0.20(1)	13.6	13.9
0.65	0.10(5)	0.85(8)	11.9	12.3	0.03(2)	0.10(4)	10.7	10.9
0.94	0.18(6)	0.87(8)	21.4	22.8	0.15(2)	0.84(3)	16.2	17.3

IV. DISCUSSION

First we discuss the inability to refine a split site on O(1) perpendicular to the chain. The thermal factors are enormous on this site in this direction and there is certainly lateral disorder associated with the chain oxygens. It was therefore a surprise that a split position did not improve the fit. Presumably the reason is that the chain is buckled in such a way that the oxygen ions take up a variety of displaced positions rather than two distinct displaced positions. This implies that the wavelength of the buckling is longer than two unit cells. We cannot determine if this buckling is static or dynamic. A similar argument can be made for the Cu(1) displacements in the a direction, though these are somewhat smaller than those observed on the chain oxygen ions.

We turn now to the planar copper ions. In this case a finite split is refined with an improvement in residual. Based on preceding arguments, this suggests that the distribution of Cu(2) is bimodal (Fig. 3). This might be expected if every copper site is not in the same charge state as would happen in the presence of polarons or local charge stripes in which case some sites would be Cu^{2+} and others Cu^{3+}, for example. Cu(2) sits at the base of a pyramidal cap of oxygen ions and does not lie on a center of symmetry; this is in contrast to the copper in single layer materials where it is octahedrally coordinated. In the present case, in response to increasing its charge state, the copper might be expected to change its position in such a way so as to move towards the negative oxygen ions: Cu^{3+} is expected to move into the oxygen pyramid somewhat. This is seen in the average structure as a function of oxygen concentration. The average Cu(2)-O(4) bond length changes from 2.4421 Å to 2.2708 Å on going from $x=0.1$ to $x=0.94$. This effect is also seen in XAFS.[33] The difference in these two bond lengths is 0.1713 Å which is a similar magnitude to the observed split Δ. If there are charge inhomogeneities in the CuO_2 plane, copper ions with different Cu(2)-O(4) bond lengths will coexist. In the absence of long-range order this will only be evident directly in the local structure, though an elongated thermal factor will be apparent crystallographically. Thus, the PDF results are consistent with crystallographic observations of an enlarged Cu(2) U_{33} (Refs. 9,12, and 13) (at least on underdoped samples[9]). Recently, yttrium XAFS results also point towards a Cu(2) site split along the c direction.[34] In this case the split is smaller (0.05 Å) and is correlated with displacements of O(2) and O(3) and probably the whole pyramid of O(2,3,4). However, the disagreement with this study in the size of the split is probably not significant given the uncertainty of both measurements. It would be interesting to model correlated atom displacements; however, we plan to collect data with better statistics or differential PDF data before attempting this. Correlated displacements of Cu(2) in directions out of the plane are also

consistent with the presence of diffuse scattering in electron diffraction.[35] We also note that there is independent evidence for disorder on copper sites which may be correlated with the charge-state of the copper. Ion-channeling experiments[36] found an anomaly in the Y-Ba-Cu signal in superconducting 123 around T_c but not in the Y-Ba signal of the same sample.

The motivation for this study was to see whether doping induces a double-well potential at the apical oxygen site as suggested from earlier XAFS work. Our results clearly rule out a local split site for O(4) along *c*. However, we note that our findings are not necessarily in contradiction with the XAFS results. This can be understood as follows: In an XAFS experiment the neighborhood of a particular atomic species is probed. The single-scattering paths correspond to pair distance distributions similarly as observed from PDF. However, one of the atoms in the pair is the photoabsorber. If a distance appears split, it is therefore not unique which of the two atoms in the pair sits on a split site. Thus, in the present case the beat observed in the Cu XAFS (Ref. 6) may possibly be explained by a split position on Cu(2). In principle this could be resolved by investigating the pair correlations between other atoms too. In practice this is difficult since typically in the XAFS data analysis multiple-scattering paths involving triple- and higher-scattering paths contribute significantly beyond the first two nearest-neighbor peaks. The multiple-scattering paths are generally difficult to take into account and their number grows rapidly with increasing distance from the photoabsorber. We also note that the XAFS signal is affected by the valence of the photoabsorber ion. We are not aware of an analysis of the XAFS data which takes into account the possibility that some Cu sites are 2+ and others 3+. This might also help to reconcile the XAFS and diffraction work.

It is interesting that refinement of the Cu(2) split position is more robust when a narrower range of *r* is fit. This suggests that even by 15 Å the structure resembles the average structure. This suggests that any charge inhomogeneities are atomic scale and there is no evidence of even nanometer-scale charge phase separation. At optimal doping we would expect ~15% of Cu sites to contain holes.[37] In the stripe model[1,3] the distance of closest approach of these holes would be ~5.4 Å and the separation of stripes would be ~16 Å.[3] Atomic pair correlations originating in one stripe and terminating in an adjacent one will more resemble the average structure than the local configuration either in a charge stripe or between stripes. Our PDF results support charge inhomogeneities on this atomic length scale rather than some kind of longer-length-scale phase separation.

Local structural inhomogeneities in $La_{2-x}Sr_xCuO_4$ (Ref. 2) disappear in the overdoped state. This coincides with the point where the pseudogap transition T_p merges with T_c. The suggestion is that below T_p the charge dynamics is from fluctuating localized charges whereas above T_p the carriers are delocalized and electronically induced structural inhomogeneities go away.[38] We note that T_p falls rapidly to T_c between $x=0.95$ and $x=1.0$.[39] The optimum doping level is sometimes inferred by the value of T_c only and the oxygen content is not well characterized. However, T_c versus doping is quite flat around optimum doping. A sample with a true doping level which falls slightly below optimum doping would be in the underdoped regime and therefore exhibit structural distortions. A slightly overdoped sample on the contrary would not exhibit structural distortions. This might explain the fact that for samples around optimal doping there is some disagreement about the existence or otherwise of local structural distortions.[15,16]

The presence of atomic-scale charge inhomogeneities in the CuO_2 planes is presently emerging as a common feature of high-T_c cuprates. Inhomogeneous local bucklings of the Cu-O bond have been observed in $La_{2-x}Sr_xCuO_4$ (Refs. 2 and 3 and $Nd_{2-x}Ce_xCuO_4$.[24,40] Recently stripes have been observed in hole-doped 214 cuprates.[1] Our results suggest that such inhomogeneities are also present in $YBa_2Cu_3O_{6+x}$. In the present analysis we address only the question whether sites are split or not and not the possibility of short-range ordered patterns of atomic displacements in the chains and planes.[34,35] The existence of stripes cannot be invoked directly from our analysis. However, they can be interpreted as being due to the presence of atomic-scale charge inhomogeneities consistent with the presence of a dynamic local stripe phase.

V. CONCLUSIONS

From our pair distribution analysis on $YBa_2Cu_3O_{6+x}$ ($x=0.25$, 0.45, 0.65, 0.94) we find no evidence for a split apical oxygen site. A finite split of the order 0.1 Å obtained for the in-plane Cu(2) along *c* resulted in an improvement of the fit over the average crystallographic model. The origin of such a split can be explained assuming the presence of both Cu^{2+} and Cu^{3+} in the CuO_2 planes as might be expected in the presence of charge stripes or polarons.

ACKNOWLEDGMENTS

We would like to thank V. Petkov, Th. Proffen, and T. A. Tyson for invaluable discussions and J. Johnson for her help with GLAD data collection. This work was supported by the NSF through Grant No. DMR-9700966. M.G. acknowledges support from the Swiss National Science Foundation. The IPNS is funded by the U.S. Department of Energy under Contract No. W-31-109-Eng-38 and the MLNSC under Contract No. W-7405-ENG-36.

[1] J.M. Tranquada, B.J. Sternlieb, J.D. Axe, Y. Nakamura, and S. Uchida, Nature (London) **375**, 561 (1995).

[2] E. Božin, S.J.L. Billinge, G.H. Kwei, and H. Takagi, cond-mat/9907017 (unpublished).

[3] E.S. Božin, S.J.L. Billinge, G.H. Kwei, and H. Takagi, Phys. Rev. B **59**, 4445 (1999).

[4] A. Bianconi, N.L. Saini, A. Lanzara, M. Missori, T. Rossetti, H. Oyanagi, H. Yamaguchi, K. Oka, and T. Ito, Phys. Rev. Lett. **76**, 3412 (1996).

[5] S.D. Conradson and I.D. Raistrick, Science **243**, 1340 (1989).

[6] J. Mustre-de Leon, S.D. Conradson, I. Batistić, and A.R. Bishop, Phys. Rev. Lett. **65**, 1675 (1990).

[7] J. Mustre de Leon, S.D. Conradson, I. Batisić, A.R. Bishop, I.D. Raistrick, M.C. Aronson, and F.H. Garzon, Phys. Rev. B **45**, 2447 (1992).
[8] J.D. Sullivan, P. Bordet, M. Marezio, K. Takenaka, and S. Uchida, Phys. Rev. B **48**, 10 638 (1993).
[9] P. Schweiss, W. Reichardt, M. Braden, G. Collin, G. Heger, H. Claus, and A. Erb, Phys. Rev. B **49**, 1387 (1994).
[10] M. François, A. Junod, K. Yvon, A.W. Hewat, J.J. Capponi, P. Strobel, M. Marezio, and P. Fischer, Solid State Commun. **66**, 1117 (1988).
[11] A. Williams, G.H. Kwei, R.B. Von Dreele, A.C. Larsen, I.D. Raistrick, and D.L. Bish, Phys. Rev. B **37**, 7960 (1988).
[12] G.H. Kwei, A.C. Larson, W.L. Hults, and J.L. Smith, Physica C **169**, 217 (1990).
[13] G.H. Kwei, A.C. Lawson, W.L. Hults, and J.L. Smith, Physica C **175**, 615 (1991).
[14] T. Egami and S.J.L. Billinge, Prog. Mater. Sci. **38**, 359 (1994).
[15] E.A. Stern, M. Qian, Y. Yacoby, S.M. Heald, and H. Maeda, Physica C **209**, 331 (1993).
[16] C.H. Booth, F. Bridges, G.J. Snyder, and T.H. Geballe, Phys. Rev. B **54**, R15 606 (1996).
[17] T.A. Tyson, J.F. Federici, D. Chew, A.R. Bishop, L. Furenlid, W. Savin, and W. Wilber, Physica C **292**, 163 (1997).
[18] T. Egami and S. J. L. Billinge, in *Physical Properties of High-Temperature Superconductors V*, edited by D. M. Ginsberg (World Scientific, Singapore, 1996).
[19] T. Egami, in *Local Structure from Diffraction*, edited by S. J. L. Billinge and M. F. Thorpe (Plenum, New York, 1998), p. 1.
[20] S.I. Zabinsky, A. Ankudinov, J.J. Rehr, and R.C. Albers, Phys. Rev. B **52**, 2995 (1995).
[21] Th. Proffen and S. J. L. Billinge (unpublished).
[22] S. J. L. Billinge, in *Physics of Manganites*, edited by T. A. Kaplan and S. D. Mahanti (Plenum, New York, 1999), p. 201.
[23] K. Kishio, T. Hasegawa, K. Suzuki, K. Kitazawa, and K. Fueki, in *High Temperature Superconductors: Relationships between Properties, Structure, and Solid-State Chemistry*, edited by J. R. Jorgensen, K. Kitasawa, J. M. Tarascon, M. S. Thompson, and J.B. Torrance, MRS Symposia Proceedings No. 156 (Materials Research Society, Pittsburgh, 1989), p. 91.
[24] S.J.L. Billinge and T. Egami, Phys. Rev. B **47**, 14 386 (1993).
[25] S. J. L. Billinge, Ph.D. thesis, University of Pennsylvania, 1992.
[26] B.H. Toby and T. Egami, Acta Crystallogr., Sect. A: Found. Crystallogr. **48**, 336 (1992).
[27] E. Prince, *Mathematical Techniques in Crystallography and Materials Science* (Springer-Verlag, New York, 1982).
[28] A. C. Larson and R. B. Von Dreele (unpublished).
[29] H. Shaked, P. M. Keane, J. C. Rodriguez, F. F. Owen, R. L. Hitterman, and J. D. Jorgensen, editors, *Crystal Structures of the High-T_c Superconducting Copper Oxides* (Elsevier Science, Amsterdam, 1994).
[30] This value is different from that shown in Table I (though they agree within the errors) because the Rietveld and single-crystal refinements were carried out with slightly different constraints on thermal factors. Results of all Rietveld and PDFFIT refinements are available on request from the authors.
[31] B.H. Toby and T. Egami, Acta Crystallogr., Sect. A: Found. Crystallogr. **48**, 163 (1992).
[32] D. Louca, G. H. Kwei, B. Dabrowski, and Z. Bukowski, Phys. Rev. B **60**, 7558 (1999).
[33] J. Röhler, P.W. Loeffen, K. Conder, and E. Kaldis, Physica C **282-287**, 182 (1997).
[34] J. Röhler, cond-mat/9906432 (unpublished).
[35] J. Etheridge, Philos. Mag. A **73**, 643 (1996).
[36] R.P. Sharma, T. Venkatesan, Z.H. Zhuang, J.R. Liu, R. Chu, and W.K. Chu, Phys. Rev. Lett. **77**, 4624 (1996).
[37] T. Schneider and H. Keller, Phys. Rev. Lett. **69**, 3374 (1992).
[38] Y.J. Uemura, A. Keren, L.P. Le, G.M. Luke, W.D. Wu, Y. Kubo, T. Manako, Y. Shimakawa, M. Subramanian, J.L. Cobb, and J.T. Markert, Nature (London) **364**, 605 (1993).
[39] J. Demsar, B. Podobnik, J.E. Evetts, G.A. Wagner, and D. Mihailovic, Europhys. Lett. **45**, 381 (1999).
[40] A. Ignatov, J. Feldhaus, V. Chernov, and A. Ivanov, J. Synchrotron Radiat. **6**, 767 (1999).